

A COMPACT GRATING-STABILIZED DIODE LASER SYSTEM, AND A DOPPLER-FREE LASER POLARIZATION SPECTROMETER FOR Rb

Edgar Méndez M.

Facultad de Ciencias, Universidad Autónoma del Estado de México
El Cerrillo Piedras Blancas, Toluca, Edo. De México.
Tel. (722) 296 55 56, edgar@nucleares.unam.mx

Alejandro Hernández H., y José I. Jiménez M.

Instituto de Ciencias Nucleares, UNAM
Circuito Exterior s/n, Ciudad Universitaria, México, D.F.
Tel. (55) 56 22 46 72, jjimenez@nucleares.unam.mx

We describe a compact, economic and versatile diode laser system based on commercial laser diode and a collimation tube, optically stabilized by means of feedback from a diffraction grating. Detailed instructions for the construction and operation of the diode laser system are presented. These instructions include machine drawings for the parts to be constructed. Our system offers single-mode operation with a linewidth of a few MHz, continuous scan over 4 GHz. Using the diode laser system we perform a sensitive method of Doppler-free spectroscopy that we test on ^{87}Rb and ^{85}Rb vapor, monitoring the nonlinear interaction of two monochromatic laser beams in an absorbing gas via changes in light polarization. The signal-to-background ratio can greatly surpass that of saturated absorption. We show that this method provides us with a tool for evaluation of the spectral bandwidth of the grating-stabilized diode laser system.

I. INTRODUCTION

Since their first use in atomic physics in the early 80's, diode lasers have become an important part of many modern experiments. This is primarily due to the high reliability and the low price of these devices which facilitate experiments involving a number of lasers operating at different frequencies [1]. Atomic-physics experiments have strict demands on the quality of the laser system used for trapping and cooling of atoms. One of the most popular atomic species is ^{87}Rb which, for instance, can be easily cooled to quantum degeneracy. It has a cycling transition close to 780 nm, used for cooling and trapping, e.g. optical molasses and magneto-optical traps. For this wavelength, semiconductor laser-diode systems have been available for some time, due to their use in compact disk players and recorders [2]. The use of diode lasers for atom –cooling experiments have been made possible by the development of extended-cavity diode lasers (ECDL). These take advantage of the available laser diodes and use frequency-selective feedback to achieve tunability and narrow linewidth typically via a diffraction grating in either the Littrow or Littman configuration. The light diffracted from a grating is coupled back into the diode, so that the grating and the diode's rear facet form an external resonator. The diode chip, with its reflecting facets, acts like an intracavity etalon and the external

diffraction grating selects a single-mode of the chip. The use of a grating results in a linewidth reduction of two orders of magnitude and provides a linewidth reduction to the 100 kHz level which is sufficient for many experiments [3,4]. The simplicity of this stabilization arrangement has led a number of research groups to design laser systems utilizing the technique [5]. This article presents an alternative, very compact and economic mechanical design. Our setup can easily be manufactured and provides high passive stability.

2. CONSTRUCTION

The essential requirements for the extended cavity are that the laser diode, the diffraction grating, and a collimating lens all be located rigidly with respect to each other, and that the angle of the grating and the position of the lens be precisely adjustable. Our design takes advantage of the fact that these requirements can now be satisfied with convenient low-cost commercial components.

The laser design is shown in Fig. 1. The laser body consists of two thick aluminum plates connected by tree nylon screws, all mounted on a solid rectangular aluminum block (Fig. 1a).

The optics system consist essentially of two parts: a metal block, holding the laser diode and the collimating optics and a custom built kinematics mount

(Thorlabs, Inc. KMS) for the diffraction grating in a Littrow configuration (Fig. 1b). The distance between laser diode and grating is about 20 mm.

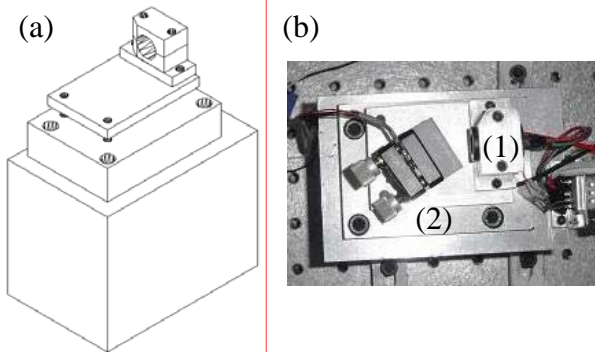


FIG. 1. (a) Schematic diagram of the extended-cavity diode laser without grating. (b) Picture of the diode laser system (Littrow configuration): (1) diode laser mount (Thorlabs LT240P-B) which also acts as a mount for the collimating lens, (2) Kinematic mount (Thorlabs KMS) for the diffraction grating.

Our standard diffraction grating for near-infrared operation is aluminum coated 1200 grooves/mm ruled diffraction grating on a 12.5x25x6 mm³ substrate (Edmund Optics Inc. NT43-209). With the light polarized parallel to the lines of the grating it provides feedback, sufficient for good tunability and stability. A pair of piezoelectric (PZT) disks is inserted between the grating mount adjustment screw and the movable face of the mount in order to rotate the grating about a vertical axis and alter the cavity length with electrical control providing fine adjustment of the cavity length for scanning the laser frequency.

A collimation tube (Thorlabs, Inc. LT240P-B) holds the laser diode and the collimating lens (an aspheric optic with $f=6.2$ mm and $NA=0.4$). The threaded tube also provides precisely adjustable focusing of the collimating lens, and it accurately locates the collimating lens axis along the laser diode axis.

An advantage of the compact cavity design is that it is easy to control the temperature of the complete laser using a Peltier thermoelectric cooler (TEC). To this end, a small hole is drilled in the mirror mount near the diode, and a thermistor is glued inside it. A Peltier thermoelectric cooler, with 9W of cooling power, is placed between the two aluminum plates. The lower plate is attached to the principal block, which acts a heatsink. This

arrangement allows precise adjustment of the diode temperature without affecting the length of the laser cavity.

Alignment of the completed laser proceeds as follows. The laser diode is mounted in the collimation tube. The linear polarization of the output light (which is parallel to the minor axis of the elliptical beam facet) is aligned vertically. The divergence of the laser beam is corrected through a collimation lens. The position and orientation of the collimator must be carefully adjusted in order to optimize the final laser performance. The collimating lens should not be tilted with respect to the laser axis in order to minimize additional astigmatism. The distance between the lens and the laser diode is adjusted so that the output beam is well collimated. This can be achieved by minimizing the laser beam diameter at a distance of several meters away from the diode. The grating mount is bolted to the main block after rough orientation such that two distinct, nearly parallel light beams emerge from the grating and the long axis of the elliptical laser beam is perpendicular to the lines on the grating. The brighter beam is the zeroth order reflection of the beam incident on the grating. The second weaker beam results from the first diffraction order, back reflected by the diode. To align the grating we use an iterative procedure. We begin by setting the injection current such that the diode laser operates slightly below threshold where the diode is most sensitive to feedback, as it cannot lase by itself. By means of both the adjustment screws, the two fluorescence beams emerging from the grating are brought together until they roughly overlap. This should yield a sudden increase of the brightness of the emission resulting from the fact that laser action has started. The injection current is then reduced until the lasing action disappears and the alignment is repeated. A sufficiently good alignment is characterized by a decrease of the threshold current by about 10-15% as compared to the threshold current of the free-running diode. Adjusting the grating angle and the focusing of the collimating lens can optimize the output power. The lens adjustment is very critical, corresponding to only a few degrees of rotation of the lens. Once the system is lasing, the laser current can be increased to give the desired output power, and the horizontal grating adjustment is used to tune to the required wavelength.

The output beam is the zeroth-order specular reflection from the grating and contained 50% of the running power. Since the external cavity is very sensitive to back reflections of the output beam, an optical isolator is used for the output beam. The

temperature is held at approximately 15°C at all times during the measurements.

Coarse adjustment of the wavelength is achieved by horizontally tilting the grating with the adjustment screw. This usually causes the laser to mode hop a few times in steps of 5-8 GHz (the cavity mode spacing). Continuous frequency scans (over 4 GHz) are possible by means of the grating PZT. A length change of the PZT synchronously varies the cavity length and the grating angle. The maximum scan width is limited by the fact that the ratio between longitudinal and angle adjustment of the grating is not optimal in our design, with larger continuous scans expected with appropriate synchronous translation and rotation of the grating. Much smoother tuning is expected from a laser that has a lower reflectivity output facet.

3. PERFORMANCE

We have constructed several systems using HITACHI HL7851G 785 nm 50 mW laser diodes. These devices perform well in the cavity described here and were used to obtain the performance data presented in this section.

The linewidth of the free-running laser was measured by means of polarization spectroscopy. Polarization spectroscopy is an example of a sub-Doppler spectroscopic technique with counter propagating pump and probe beams derived from the same laser. The principle of polarization spectroscopy is to induce a birefringence in a medium, with circularly polarized pump beam, and to interrogate this with a counter propagating weak probe beam. The scheme of a polarization spectrometer is shown in Fig. 2.

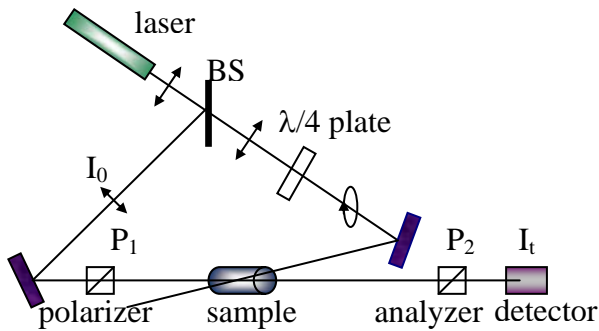


FIG. 2. Polarization spectroscopy; experimental setup.

It can be regarded as a form of saturation spectroscopy, with the change of the complex refractive index being proportional to the pump intensity, and as such is an example of third order nonlinear effect. As in conventional saturation spectroscopy, a resonant probe signal is expected only near the center of a Doppler-broadened absorption line where both beams are interacting with the same atoms, those with essentially zero axial velocity.

The polarization spectroscopy signal at the probe detector is [6]:

$$I_t(\omega) = I_0 e^{-\alpha L - \alpha_w} \left\{ \xi + \theta'^2 + \frac{1}{4} \Delta \alpha_w^2 + \theta' \Delta \alpha_0 L \frac{x}{1+x^2} + \left[\frac{\Delta \alpha_0 \Delta \alpha_w L}{4} + \left(\frac{\Delta \alpha_0 L}{4} \right)^2 \right] \frac{1}{1+x^2} + \frac{3}{4} \left(\frac{\Delta \alpha_0 x}{(1+x^2)} \right)^2 \right\} \quad (1)$$

with $x = \frac{\omega_0 - \omega}{\gamma_s / 2}$, where ω_0 is the center frequency of

the atomic transition, and γ_s is the homogeneous width of the atomic transition saturated by the pump wave. The signal contains a constant background term $\xi + \theta'^2 + \Delta \alpha_w^2 / 4$ that is independent of the frequency ω . The quantity $\xi = I_t / I_0$ gives the residual transmission of the completely crossed analyzer P_2 . The third term is due to the absorption part of the windows birefringence. All these three terms are approximately independent of the frequency ω .

The next three terms contribute to the line profile of the polarization signal. The first frequency-dependence term in (1) gives the additional transmitted intensity when the angle $\theta' = \theta + (\omega / 2c) \Delta b_r$ is not zero, where θ is the angle which the transmission axis of the analyzer P_2 is tilted, and b_r is the real part of the refractive index of the absorption cell windows. This term has a dispersion-type profile. For $\theta' = 0$ the dispersion term vanishes.

The two Lorentzian terms depend on the product of $\Delta \alpha_w$ and $\Delta \alpha_0 L$ and on $(\Delta \alpha_0 L)^2$, where L is the path length through the pumped region of the sample and $\Delta \alpha_0$ is the difference between absorption coefficients

of the induced birefringent gas sample. By squeezing the windows their dichroism (that is, $\Delta\alpha_w$) can be increased and the amplitude of the first Lorentzian term can be enlarged. Of course, the background term $\Delta\alpha_w^2$ also increases and one has to find the optimum signal-to-noise ratio. Since in most cases $\Delta\alpha_0 L \ll 1$, the last term in (1), which is proportional to $\Delta\alpha_0^2 L^2$, is generally negligible. Nearly pure dispersion signals can be obtained if $\Delta\alpha_w$ is minimized and θ' is increased until the optimum signal-to-noise ratio is achieved. Therefore by controlling the birefringence of the window either dispersion-shaped or Lorentzian line profiles can be obtained for the signals.

Typically experimental results are shown in Figure 3. The data were taken with a pump power of 840 μ W, and a probe power of 120 μ W. The upper trace shows the polarization spectrum. The trace b) plots the saturated absorption signal as a function of laser frequency. Zero detuning is relative to the $F = 3 \rightarrow F' = 4$ transition in ^{85}Rb . The saturated absorption/hyperfine pumping spectrum for the transition $F = 3 \rightarrow F'$ in ^{85}Rb , and $F = 2 \rightarrow F'$ in ^{87}Rb are seen. As a reference, the trace c) plots the absorption through the cell as a function of laser frequency. The trace a) is the difference between the traces b) and c). The polarization signals for the closed transitions $F = 3 \rightarrow F' = 4$ in ^{85}Rb and $F = 2 \rightarrow F' = 3$ in ^{87}Rb are expected to be the largest - this is seen clearly in the figure 3.

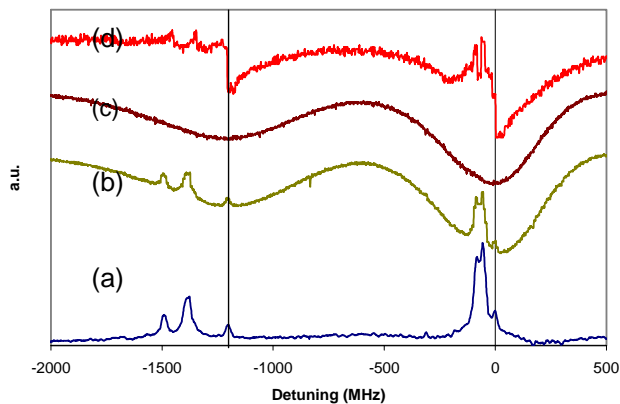


FIG 3. Typical experimental results. The upper trace shows the polarization spectrum. The trace (b) is the saturated absorption spectrum for the transition $F=2 \rightarrow F'$ in ^{87}Rb and for $F=3 \rightarrow F'$ in ^{85}Rb . The trace (c) is the absorption spectrum and the trace (a) is the difference between (b) and (c).

To estimate the expected linewidth of the extended-cavity diode laser we use the equation for a cavity linewidth [7]:

$$\Delta\lambda \approx \frac{\Delta\theta}{F (\partial\theta/\partial\lambda)}$$

where $\Delta\theta$ is the beam divergence, $\partial\theta/\partial\lambda$ is the intracavity dispersion and F is the total cavity finesse. The beam divergence has the form $\Delta\theta \approx \lambda/\pi w$ [8], where λ is the emission wavelength and w is the beam waist. From the grating equation we have $\partial\theta/\partial\lambda = 1/d \cos\theta$. The extended-cavity finesse is the product of the diode laser active region finesse and the external cavity finesse. With $\lambda \approx 780\text{nm}$, $w \approx 1.4\text{mm}$, and $F \approx 600$, the expected linewidth is 9 MHz.

In our experiment the polarization spectrum has a dispersion-type profile (figure 3d). For the transitions $F \rightarrow F'=F+1$ the dispersion signal is proportional to the derivative of the saturated absorption signal [8]. The dispersion signal has high slope crossing the center of the resonance and as a first approximation we suppose that the frequency difference between the maximum and minimum points of the dispersion signal is an upper limit for the emission linewidth. Using the polarization spectrum in figure 3d we estimate that the experimental linewidth is 10 MHz.

ACKNOWLEDGEMENT

The development of this laser system was done in the "Virgilio Beltrán" laboratories at ICN, UNAM. This work was supported by CONACYT under Grant 44986 and by DGAPA, UNAM under Grant IN120806-3.

REFERENCES

- [1] T. Meijer, J. D. White, B. Smeets, M. Jeppesen, and R. E. Scholten, "Blue five-level frequency-upconversion system in rubidium", *Opt. Lett.*, **31**, 1002-1004 (2006).
- [2] C. E. Wieman, and L. Holberg, "Using diode lasers for atomic physics", *Rev. Sci. Instrum.* **62**, 1-20 (1991).
- [3] L. Ricci, M. Weidenmüller, T. Esslinger, A. Hemmerich, C. Zimmermann, V. Vuletic, W. König, and T. W. Hänsch, "A compact grating stabilized diode laser system for atomic physics", *Opt. Commun.* **117**, 541-549 (1995).
- [4] K. B. MacAdam, A. Steinbach, and C. Wieman, "A narrow-band tunable diode laser system with grating feedback, and a saturated absorption spectrometer for Cs and Rb", *Am. J. Phys.* **60**, 1098-1111 (1992).

- [5] A. S. Arnold, J. S. Wilson, and M. G. Boshier, "A simple extended-cavity diode laser", *Rev. Sci. Instrum.* **69**, 1236-1239 (1998).
- [6] Demtröder W., *Laser Spectroscopy*, 2nd ed., Berlin: Springer, 1998.
- [7] F. P. Schäfer, Ed., *Dye Laser*, 2nd revised edition, Topics in Applied Physics, Vol. 1, Springer-Verlag, Berlin, 1977.
- [8] Davis C. C., *Laser and Electro-Optics*, Cambridge University Press, 349-354, 2000.
- [9] Jing Zhang, Dong Wei, Changde Xie, and Kunchi Peng, "Characteristics of absorption and dispersion for rubidium D₂ lines with the modulation transfer spectrum", *Optics Express* **11**, 1338-1344 (2003).